

# The two-mode Bose-Hubbard model revisited: Many-particle and mean-field evolution in phase space

F. Trimborn, D. Witthaut and H. J. Korsch

*FB Physik, Technische Universität Kaiserslautern, D-67653 Kaiserslautern, Germany*

(Dated: February 9, 2022)

The number-conserving quantum phase space description of the Bose-Hubbard model is discussed for the simple but illustrative case of two modes. We introduce the Husimi- $(Q)$  and the Glauber-Sudarshan- $(P)$ -distribution function and show that they provide a distinguished tool to analyze many-particle quantum states. The exact evolution of these distribution functions are given by second-order partial differential equations, which they provide a distinguished instrument to derive the celebrated mean-field limit and to go beyond this approximation. An important consequence is that the applicability of the mean-field dynamics is greatly enhanced by considering classical phase space distributions or ensembles instead of single trajectories. Two important applications of this approach are discussed in detail. For instance this method cures the well-known breakdown of the mean-field approximation when the classical dynamics becomes unstable. Furthermore we discuss the heating of a BEC due to elastic scattering with the background gas which can be understood simply as phase noise.

PACS numbers: 03.75.Lm, 03.65.-w

## I. INTRODUCTION

The physics of ultracold atoms in optical lattices has made an enormous progress in the last decade, since it an excellent model system for a variety of fields such as nonlinear dynamics or condensed matter physics. The dynamics of bosonic atoms can be described by the celebrated Bose-Hubbard Hamiltonian, which is a paradigmatic model for the study of strongly correlated many-body quantum systems [1]. Such systems are hard to deal with theoretically since the dimension of the respective Hilbert space increases exponentially both in the particle number and in the number of lattice sites. However, things can become surprisingly simple if the atoms undergo Bose-Einstein condensation. In many situations, the mesoscopic dynamics of a Bose-Einstein condensate (BEC) is extremely well described by the (discrete) Gross-Pitaevskii equation (GPE) for the macroscopic wavefunction of the condensate (see, e.g., [2]). This mean-field description is often called 'classical' since it can be viewed as the classical limit of the second quantization with the inverse particle number taking the role of  $\hbar$ . In practice, this approximation is often derived within a Bogoliubov approach, factorizing the expectation values of products of operators into the product of expectation values.

A systematic and illuminative approach to the mean-field limit is provided by a quantum phase space approach. In this formulation, a quantum state is described by a quasi-density on the corresponding 'classical' phase space, which is given by the parameter space of the generalized coherent states. This exact representation does not only give an illustrative insight into the dynamics but also allows for a deeper analysis of the many-particle-mean-field correspondence, since in the macroscopic limit of large particle numbers the distribution function of a pure Bose-Einstein condensate reduces to a point in the

'classical' phase space propagating according to the classical equation of motion – the discrete Gross-Pitaevskii equation.

The phase space formulation of quantum mechanics is nearly as old as the theory itself. Although this theory is well-established by now, only a small fraction of the literature is dedicated to systems with intrinsic symmetries and a general algorithm to construct phase space distribution functions for such system has been developed only eight years ago [3]. In the present case, we must take into account the  $SU(M)$  symmetry of the Bose-Hubbard Hamiltonian,  $M$  being the number of lattice sites, and the resulting conservation of the particle number. The correspondence of the quantum and the classical system is established by the generalized  $SU(M)$  coherent states, which incorporate the fixed particle number. The parameter space of these states and correspondingly the classical phase space are given by a multidimensional Bloch-sphere. Furthermore, the  $SU(M)$  coherent states are equivalent to the fully condensed product states and are thus of high physical significance.

In a preceding paper [4] we have surveyed the mathematical foundations of the number conserving phase space description of the Bose Hubbard model and derived the exact evolution equations for the Husimi  $Q$ -function and the Glauber-Sudarshan  $P$ -function. In the present paper we will illustrate this approach and discuss possible applications for the simple case of a two-mode Bose-Hubbard model given by the Hamiltonian

$$\hat{H} = -\Delta \left( \hat{a}_1^\dagger \hat{a}_2 + \hat{a}_2^\dagger \hat{a}_1 \right) + \epsilon \left( \hat{a}_2^\dagger \hat{a}_2 - \hat{a}_1^\dagger \hat{a}_1 \right) + \frac{U}{2} \left( \hat{a}_1^{\dagger 2} \hat{a}_1^2 + \hat{a}_2^{\dagger 2} \hat{a}_2^2 \right), \quad (1)$$

which commutes with the particle number operator  $\hat{N} = \hat{a}_1^\dagger \hat{a}_1 + \hat{a}_2^\dagger \hat{a}_2$ . Such a two-mode system was realized experimentally by confining a BEC in a double-well trap

[5, 6, 7]. Furthermore, this model can describe the fundamental phenomena of two weakly coupled BECs in more general setups [8]. Early theoretical studies of the system dynamics were reported in [9, 10].

The algebraic structure of the model are clarified by a Jordan-Wigner transformation, so that we rewrite the dynamics in terms of the operators

$$\begin{aligned}\hat{J}_x &= \frac{1}{2} \left( \hat{a}_1^\dagger \hat{a}_2 + \hat{a}_2^\dagger \hat{a}_1 \right) \\ \hat{J}_y &= \frac{i}{2} \left( \hat{a}_1^\dagger \hat{a}_2 - \hat{a}_2^\dagger \hat{a}_1 \right) \\ \hat{J}_z &= \frac{1}{2} \left( \hat{a}_2^\dagger \hat{a}_2 - \hat{a}_1^\dagger \hat{a}_1 \right),\end{aligned}\quad (2)$$

which form an angular momentum algebra  $su(2)$  with quantum number  $j = N/2$  [9, 10, 11]. The Hamiltonian (1) then can be rewritten as

$$\hat{H} = -2\Delta \hat{J}_x + 2\epsilon \hat{J}_z + U \hat{J}_z^2 \quad (3)$$

up to a constant term. This formulation makes the symmetries of the system most obvious: The angular momentum operators obviously commute with the Casimir operator, which is given by the total particle number through  $\hat{J}^2 = \hat{N}/2 (\hat{N}/2 + 1)$ . A fixed particle number thus corresponds to a fixed modulus of the angular momentum.

## II. NUMBER CONSERVING PHASE SPACE DESCRIPTION

The number conserving phase space description of the Bose-Hubbard dynamics has been introduced in [4], starting from the generalized coherent states of Gilmore [12] and Perelomov [13]. Here we will only recall the main results for the special case of two modes for the sake of completeness.

Generalized coherent states for arbitrary dynamical Lie groups are defined by the action of a translation operator onto a reference state. For instance, the celebrated Glauber coherent states for the Heisenberg-Weyl group  $H_4$  are defined by the relation  $|\alpha\rangle = \hat{D}(\alpha)|0\rangle = e^{\alpha \hat{a}^\dagger - \alpha^* \hat{a}}|0\rangle$ , where the reference state is just the vacuum state. The parameter space of the translation operators  $\hat{D}(\alpha)$  and thus the space of the coherent states is isomorphic to the classical phase space  $\mathbb{C} \simeq \mathbb{R} \times \mathbb{R}$ .

The situation is different for a BEC in double well trap since the dynamical group is now  $SU(2)$  spanned by the angular momentum operators (2). This reflects the existence of a conserved quantity, the total number of particles  $\hat{N}$ . Thus the corresponding classical phase space is not flat but given by the Bloch sphere  $\mathcal{S}^2$ . In physical terms, the  $z$ -component of the Bloch vector describes the population imbalance of the two modes, while the polar angle represents the relative phase. Since this variable is cyclic and not defined if all particles are in a single well (i.e. at the poles), the topology is clearly that of a sphere.

The  $SU(2)$  coherent states or Bloch coherent states are then defined by the action of a rotation operator onto the reference state  $|N, 0\rangle$ :

$$\begin{aligned}|\theta, \phi\rangle &= \hat{R}(\theta, \phi)|N, 0\rangle \\ &= e^{-i\theta(\hat{J}_x \sin \phi - \hat{J}_y \cos \phi)}|N, 0\rangle \\ &= \sum_{n_1+n_2=N} \binom{N}{n_2} \cos\left(\frac{\theta}{2}\right)^{n_1} \sin\left(\frac{\theta}{2}\right)^{n_2} e^{-in_2\phi} |n_1, n_2\rangle.\end{aligned}\quad (4)$$

Again the space of rotations  $\hat{R}(\theta, \phi)$  and thus the space of coherent states is isomorphic to the classical phase space  $\mathcal{S}^2$ . Instead of a parametrization of the coherent states by the angles  $\theta$  and  $\phi$  we will frequently use the variables

$$p = \cos^2(\theta/2) \quad \text{and} \quad q = \phi, \quad (5)$$

where  $p$  is the population in the second well and  $q$  the relative phase of the two modes. Note that the  $SU(M)$  coherent states are the product states, i.e. they represent a pure condensate. For two modes,  $M = 2$ , this relation simply reads

$$|\theta, \phi\rangle = \frac{1}{\sqrt{N!}} \left( \cos\left(\frac{\theta}{2}\right) a_1^\dagger + \sin\left(\frac{\theta}{2}\right) e^{-i\phi} a_2^\dagger \right)^N |0, 0\rangle. \quad (6)$$

With the help of the  $SU(2)$  coherent states one can readily introduce quasi phase space distributions of a BEC in a double well trap. The Glauber-Sudarshan  $P$ -distribution is defined as the diagonal representation of the density operator  $\hat{\rho}$  in coherent states

$$\hat{\rho} = \int_{\mathcal{S}^2} P(\Omega) |\Omega\rangle \langle \Omega| d\mu(\Omega) \quad (7)$$

where  $\Omega$  denotes the solid angle and  $d\mu(\Omega) = (N + 1)/4\pi d\Omega$  is the invariant measure on the sphere. Due to the overcompleteness of the coherent states, the  $P$ -function does always exist but is usually not unique. Furthermore it is not positive definite and often highly singular. On the other hand, the Husimi  $Q$ -function defined as the expectation value of the density operator in coherent states,

$$Q(\Omega) = \langle \Omega | \hat{\rho} | \Omega \rangle, \quad (8)$$

is unique, regular and positive definite. Thus the  $Q$ -function is especially suited for illustrations, while both quasi distribution functions will be used for actual calculations. Note, however, that the  $Q$ -function is also not a proper distribution function since it does not give the correct marginal distributions. Note that it is much harder to define the Wigner function on a spherical phase space than the  $P$ - and  $Q$ -function, since its construction uses harmonic functions on the respective phase space. This makes actual calculations hard for two lattice sites corresponding to  $SU(2)$  (see, e.g., the contradictory results in [14] and [15]) and almost impossible for larger systems.

Evolution equations for the classical phase space distributions can be derived using the mapping of operators

in Hilbert space to differential operators on the classical phase space. The  $\mathcal{D}^\ell$ -algebra representation of an arbitrary hermitian operator  $\hat{A}$  is defined in a way that both operators have the same effect when acting on a coherent state projector:

$$\hat{A}|\Omega\rangle\langle\Omega| \stackrel{\dagger}{=} \mathcal{D}^\ell(\hat{A})|\Omega\rangle\langle\Omega| \quad (9)$$

$$|\Omega\rangle\langle\Omega| \hat{A} \stackrel{\dagger}{=} \mathcal{D}^\ell(\hat{A})^*|\Omega\rangle\langle\Omega|. \quad (10)$$

The  $\mathcal{D}^\ell$ -algebra representation is well known for the Heisenberg-Weyl algebra. It has been introduced for the  $su(M)$ -algebra by Gilmore and coworkers (see [12] and references therein). The evolution equations for the  $Q$ -function are then given by

$$\begin{aligned} \frac{\partial}{\partial t}Q(\Omega) &= \text{tr}(\dot{\rho}|\Omega\rangle\langle\Omega|) \\ &= -i\text{tr}(\hat{\rho}\hat{H}|\Omega\rangle\langle\Omega| - |\Omega\rangle\langle\Omega|\hat{H}\hat{\rho}) \quad (11) \\ &= -i(\mathcal{D}^\ell(\hat{H}) - \mathcal{D}^\ell(\hat{H})^*)Q(\Omega). \end{aligned}$$

For the  $P$ -function we need an associated  $\tilde{\mathcal{D}}^\ell$ -algebra defined by an integration by parts:

$$\begin{aligned} \int_{\mathcal{S}^2} P(\Omega)\mathcal{D}^\ell(H)|\Omega\rangle\langle\Omega| d\mu(\Omega) = \\ \int_{\mathcal{S}^2} \tilde{\mathcal{D}}^\ell(H)P(\Omega)|\Omega\rangle\langle\Omega| d\mu(\Omega) \quad (12) \end{aligned}$$

Using this algebra, the evolution equation for the  $P$ -function can be derived via

$$\begin{aligned} \dot{\rho} &= \int_{\mathcal{S}^2} \frac{\partial}{\partial t}P(\Omega)|\Omega\rangle\langle\Omega| d\mu(\Omega) \quad (13) \\ &= \int_{\mathcal{S}^2} i\left(\tilde{\mathcal{D}}^\ell(H) - \tilde{\mathcal{D}}^\ell(H)^*\right)P(\Omega)|\Omega\rangle\langle\Omega| d\mu(\Omega). \end{aligned}$$

The  $\mathcal{D}^\ell$ -algebra representation of the relevant operators and the evolution equation for the  $M$ -site Bose-Hubbard-Hamiltonian have been calculated in the first part of this work [4]. Here, we just quote the exact results for the  $Q$ -function in the case of two sites,

$$\begin{aligned} \frac{\partial}{\partial t}Q(p, q) &= \left\{ +2\epsilon\frac{\partial}{\partial q} \right. \quad (14) \\ &+ \Delta \left( 2\sqrt{p-p^2}\sin q\frac{\partial}{\partial p} + \frac{1-2p}{\sqrt{p-p^2}}\cos q\frac{\partial}{\partial q} \right) \\ &\left. + U \left( N(1-2p) - 2p(1-p)\frac{\partial}{\partial p} \right) \frac{\partial}{\partial q} \right\} Q(p, q), \end{aligned}$$

and the Glauber-Sudarshan  $P$ -function,

$$\begin{aligned} \frac{\partial}{\partial t}P(p, q) &= \left\{ +2\epsilon\frac{\partial}{\partial q} \right. \quad (15) \\ &+ \Delta \left( 2\sqrt{p-p^2}\sin q\frac{\partial}{\partial p} + \frac{1-2p}{\sqrt{p-p^2}}\cos q\frac{\partial}{\partial q} \right) \\ &\left. + U \left( (N+2)(1-2p) + 2p(1-p)\frac{\partial}{\partial p} \right) \frac{\partial}{\partial q} \right\} P(p, q). \end{aligned}$$

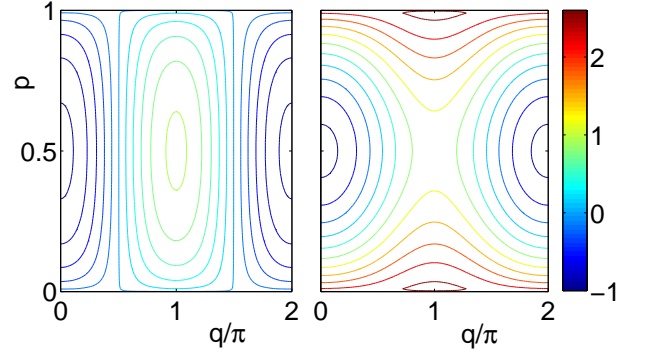


FIG. 1: Classical phase space structure: Lines of constant energy  $\mathcal{H}(p, q)$  for  $J = 1$ ,  $\epsilon = 0$ , and  $g = 0$  (left) resp.  $g = 10$  (right).

One can directly show that both evolution equations conserve the normalization. Furthermore it can be shown that the interaction terms  $\sim U$  cancel exactly for  $N = 1$ , since a single Boson obviously does not interact. The expectation values of the angular momentum operators (2) are directly given by the phase space averages [4]

$$\begin{aligned} \langle \hat{J}_k \rangle / N &= (N+2) \int_{\mathcal{S}^2} s_k(p, q)Q(p, q)d\mu(p, q) \quad \text{and} \\ \langle \hat{J}_k \rangle / N &= N \int_{\mathcal{S}^2} s_k(p, q)P(p, q)d\mu(p, q), \quad (16) \end{aligned}$$

where  $k = x, y, z$  and

$$\mathbf{s} = \begin{pmatrix} \sqrt{p(1-p)}\cos(q) \\ \sqrt{p(1-p)}\sin(q) \\ p-1/2 \end{pmatrix} \quad (17)$$

is the classical Bloch vector.

From the phase space evolution equations (14) and (15) one is directly led to the mean-field approximation in the macroscopic limit  $N \rightarrow \infty$  with  $g = UN$  fixed. In this limit one can neglect the the second order derivative terms in the evolution equations since they vanish as  $\mathcal{O}(1/N)$ . In this case one obtains a Liouville equation for a quasi-classical phase space distribution function  $\rho(p, q)$ :

$$\begin{aligned} \frac{\partial}{\partial t}\rho(p, q) &= - \left( \frac{\partial \mathcal{H}}{\partial p} \frac{\partial}{\partial q} - \frac{\partial \mathcal{H}}{\partial q} \frac{\partial}{\partial p} \right) \rho(p, q) \\ &= - \{ \mathcal{H}(p, q), \rho(p, q) \} \quad (18) \end{aligned}$$

with the Poisson bracket  $\{\cdot, \cdot\}$  and the Gross-Pitaevskii Hamiltonian function

$$\mathcal{H} = -2\epsilon p - 2\Delta\sqrt{p(1-p)}\cos(q) + \frac{g}{4}(1-2p)^2. \quad (19)$$

The macroscopic interaction strength is given by  $g = UN$  if we start from the  $Q$ -function and by  $\tilde{g} = U(N+2)$  for the  $P$ -function due to the different underlying operator ordering. The difference also vanishes in the macroscopic limit  $N \rightarrow \infty$  with  $UN$  fixed. As already mentioned,

a pure Bose-Einstein condensate, i.e. a product state, is equivalent to a  $SU(2)$  coherent state and thus its phase space representation is maximally localized. In this case one can approximate the dynamics of a phase space distribution by the dynamics of its center, which is given by the canonical equations of motion

$$\begin{aligned}\dot{p} &= -\frac{\partial \mathcal{H}}{\partial q} = -2\Delta\sqrt{p(1-p)}\sin(q) \\ \dot{q} &= \frac{\partial \mathcal{H}}{\partial p} = -2\epsilon - \Delta\frac{1-2p}{\sqrt{p(1-p)}}\cos(q) - g(1-2p).\end{aligned}\quad (20)$$

These equations are equivalent to the celebrated discrete Gross-Pitaevskii equation

$$i\frac{d}{dt}\begin{pmatrix}\psi_1 \\ \psi_2\end{pmatrix} = \begin{pmatrix}\epsilon + g|\psi_2|^2 & -J \\ -J & -\epsilon + g|\psi_2|^2\end{pmatrix}\begin{pmatrix}\psi_1 \\ \psi_2\end{pmatrix}, \quad (21)$$

if one identifies  $\psi_1 = \sqrt{1-p}$  and  $\psi_2 = \sqrt{p}\exp(-iq)$  and neglects the global phase. In the noninteracting case  $U = 0$ , these mean-field equations of motion are exact and an initially coherent state remains coherent in time. However, if one wishes to simulate the dynamics of a different initial state classically, one still has to consider phase space distribution functions instead of single trajectories.

The classical phase space structure induced by the Hamiltonian function (19) is shown in Fig. 1 for  $J = 1$ ,  $\epsilon = 0$  and two different value of the interaction strength,  $UN = 0$  and  $UN = 10$ . In the linear case one recovers the simple Rabi or Josephson oscillations. One of the elliptic fixed points bifurcates if the interaction strength exceeds the critical value  $UN = 2J$ , leading to the self-trapping effect [9, 10].

It is important to note that two steps of approximation were necessary to derive the Gross-Pitaevskii equation: In the first step we have neglected the quantum noise term in the evolution equations (14) and (15) which is always possible in the macroscopic limit  $N \rightarrow \infty$  with  $UN$  fixed. In the second step one assumes a nearly pure condensate, so that its phase space representation is strongly localized and can be approximated by a single trajectory in phase space. Thus it is possible to simulate the dynamics of *every* quantum state 'classically' up to an error of order  $1/N$  if one considers phase space distributions ensembles instead of single trajectories. The single-trajectory mean-field approximation will break down if the quantum state differs significantly from a product state while the phase space description still gives excellent results. This issue will be further discussed in Sec. IV.

Let us finally note that a comparable analysis of the dynamics of ultracold atoms in terms of a flat phase space based on Glauber coherent states has been introduced in [16]. The classical phase space is then given by  $\mathbb{C}^2$  and the distribution functions thus depend on four variables. In comparison, the present approach has some conceptual advantages as it directly embodies the conservation of the particle number  $N$  and eliminates a global phase. For

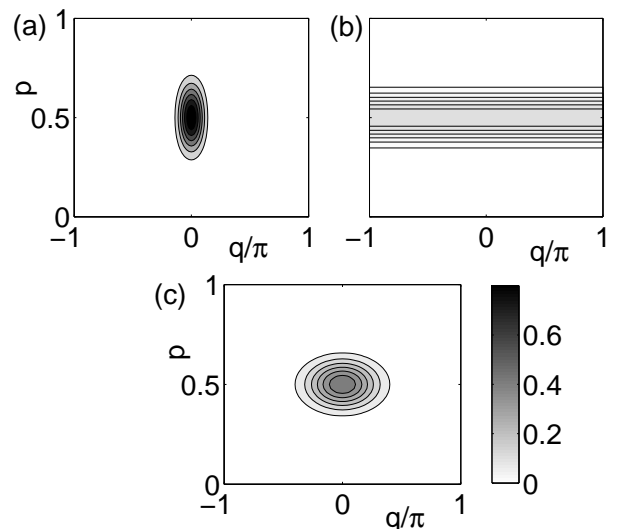


FIG. 2: Husimi functions in a Mercator projection of (a) the coherent state  $|p = 1/2, q = 0\rangle$ , (b) the Fock state  $|n_1 = N/2, n_2 = N/2\rangle$  and (c) the lowest eigenstate of the Hamiltonian (1) for  $\Delta = 1$ ,  $U = 10$  and  $\epsilon = 0$ . The number of particles is  $N = 40$  in all plots.

example the truncation of quantum noise terms in the evolution equations of the  $Q$ - and the  $P$ -function leads to an error of order  $1/N$ . In the present approach this can be directly read off from equation (14) and (15), while it is not easy to see within the Glauber phase space approach since  $N$  is an operator then and not a number. Another approach discussing the convergence to the mean-field approximation by an expansion in terms of the inverse particle number  $1/N$  has been reported in [17, 18].

### III. HUSIMI FUNCTIONS FOR THE $su(2)$ ALGEBRA

In this section we will illustrate the use of the  $SU(2)$  phase space distributions for the analysis of many-particle quantum states. Here we will restrict ourselves to the Husimi  $Q$ -function since it is always a positive, regular function and thus more suited for a graphical representation.

To become familiar with phase space distributions on the sphere we have plotted the Husimi function for (a) the coherent state  $|p = 1/2, q = 0\rangle$ , (b) the Fock state  $|n_1 = N/2, n_2 = N/2\rangle$  and (c) the lowest eigenstate of the Hamiltonian (1) for  $\Delta = 1$  and  $U = 10$  in a Mercator projection of the sphere in Fig. 2. The coherent state is maximally localized at the position  $(p, q)$  and thus closest to a point in classical phase space. On the contrary a Fock state is localized around  $p = n_2/N$ . The phase  $q$  is completely delocalized in the sense that the Husimi function is uniform in  $q$ . Finally one can clearly visualize the number squeezing of the eigenstate (c) in comparison with the coherent state (a) due to the interaction term

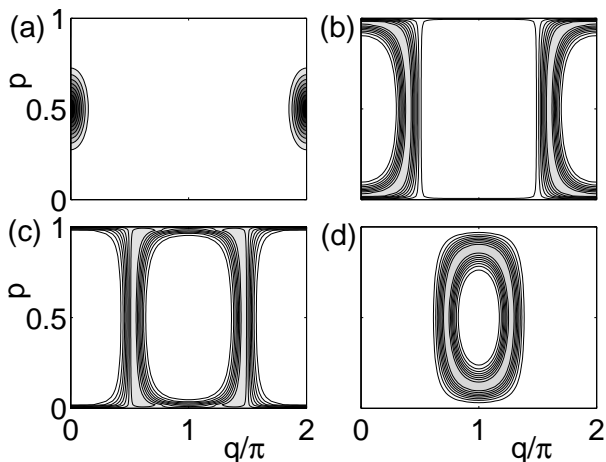


FIG. 3: Husimi density of the eigenstates  $|E_n\rangle$  with  $n = 1, 15, 23, 34$  (a-d) of the Hamiltonian (1) for  $\Delta = 1$ ,  $\epsilon = 0$ ,  $UN = 0$  and  $N = 40$  particles. Dark colors encode high values of the Husimi density.

in the Hamiltonian – a fact which is desirable for matter wave interferometer experiments [19].

Furthermore, we have plotted the Husimi function for some selected eigenstates of the Bose-Hubbard Hamiltonian (1) for the linear case  $UN = 0$  in Fig. 3 and for  $UN = 10$  in Fig. 4. The Husimi functions of the eigenstates localize on the classical phase space trajectories of the respective energy as shown in Fig. 1, where their sum covers the classical phase space uniformly,

$$\sum_n Q_{|n\rangle}(p, q) = 1. \quad (22)$$

In the linear case  $UN = 0$ , the classical trajectories correspond to the Rabi oscillations between the two wells as shown on the left hand side of Fig. 1. This behavior is directly mirrored by the eigenstates as shown in Fig. 3: The lowest eigenstate localizes on the classical fixed point  $(p, q) = (0, 0)$  while the others correspond to Rabi oscillations

The situation is more interesting, when the interaction strength exceeds the critical value for the self-trapping bifurcation, as shown exemplarily for  $UN = 10$  in Fig. 4. For low energies one still finds Rabi modes, while the eigenstates of higher energies correspond to self-trapping trajectories with a persistent particle number difference and a running phase (cf. Fig. 1, right). However, the eigenstates always localize equally on the trajectories with  $p > 1/2$  and  $p < 1/2$  because of the symmetry of the Hamiltonian (3). Most interestingly, quantum states can also localize at the unstable hyperbolic fixed point as shown in Fig. 4 (c).

Finally we would like to emphasise the fact that the Husimi function contains the complete information about the quantum state. In fact, one can reconstruct a pure state solely from the  $N$  zeros of the Husimi function or the Bargmann function up to a global phase factor [20].

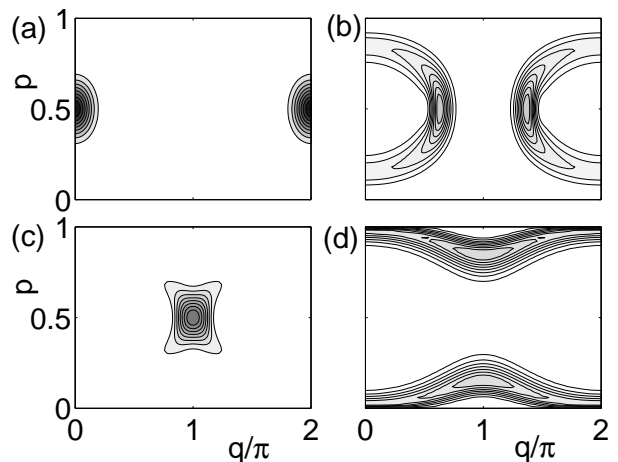


FIG. 4: As Fig. 3, however for  $UN = 10$ .

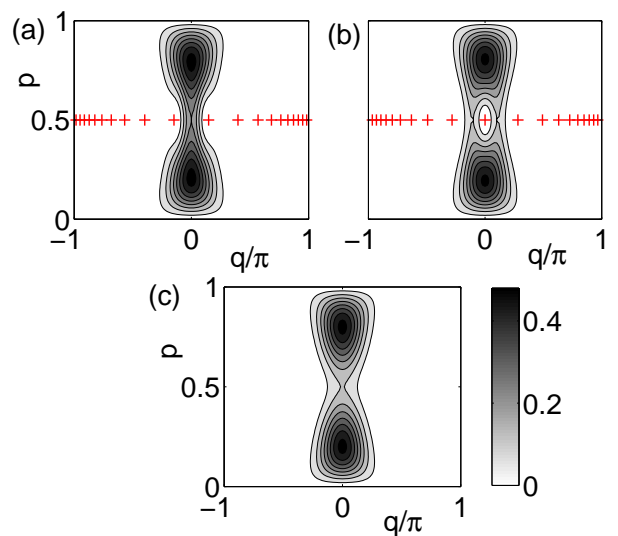


FIG. 5: (Color online) Husimi density of the cat states  $|\psi_{\pm}\rangle \propto |0.2, 0\rangle \pm |0.8, 0\rangle$  (a,b) and the incoherent sum  $\hat{\rho}_+ = (|0.2, 0\rangle\langle 0.2, 0| + |0.8, 0\rangle\langle 0.8, 0|)/2$  (c) for  $N = 20$  particles. The zeros of the Husimi function are marked by red crosses.

Thus these zeros carry the essential information about the quantum states. As an example, Fig. 5 compares the Husimi distribution of a cat state, i.e. a coherent superposition of two coherent states  $|\psi_{\pm}\rangle \propto |p = 0.2, q = 0\rangle \pm |p = 0.8, q = 0\rangle$ , with the incoherent sum of these two states  $\hat{\rho}_+ = (|0.2, 0\rangle\langle 0.2, 0| + |0.8, 0\rangle\langle 0.8, 0|)/2$ . The global shape of the Husimi function of the three states appears quite similar with significant differences only around the point  $(p, q) = (0.5, 0)$ . The Husimi density is increased (decreased) for the coherent superpositions  $|\psi_+\rangle$  ( $|\psi_-\rangle$ ) in comparison with the incoherent sum, reflecting constructive (destructive) interference. The complete information about the pure states  $|\psi_{\pm}\rangle$  is coded in the distribution of the  $N = 20$  zeros of the Husimi function, which are plotted as red crosses in the figure. The Husimi function of the mixed state  $\hat{\rho}_+$  has no zero at all.

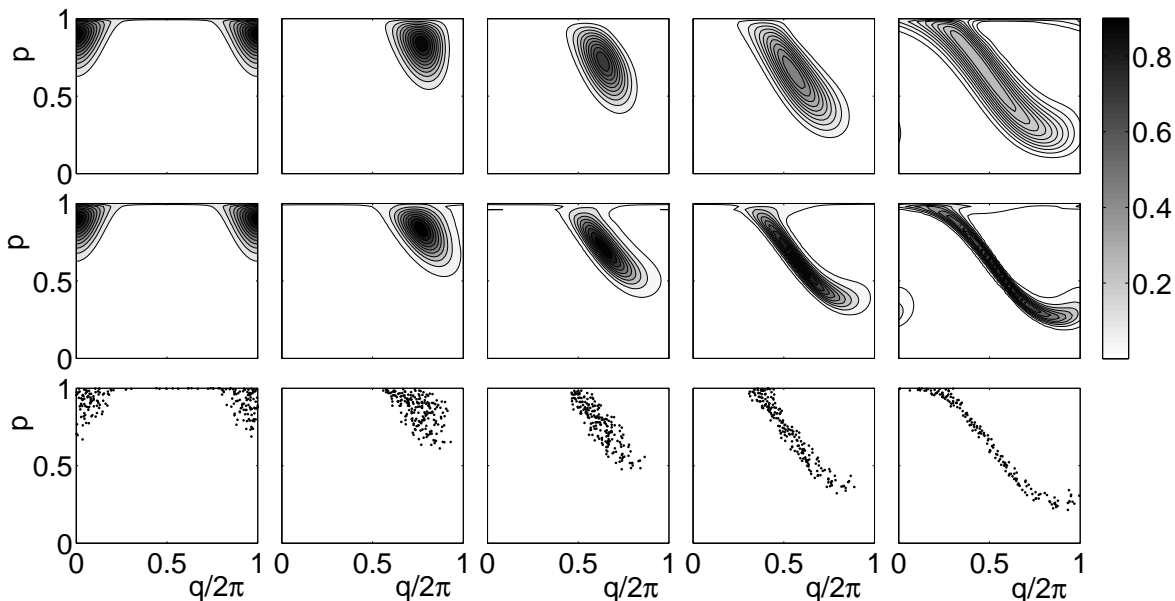


FIG. 6: Breakdown of the mean-field approximation around a hyperbolic fixed point in phase space. Shown is the dynamics of an initially coherent state located at  $p_0 = 0.9045$  and  $q_0 = 0$  at times  $t = 0, 0.12, 0.24, 0.36, 0.48$  (from left to right) for  $\Delta = 1$ ,  $UN = 10$  and  $N = 20$  particles. The exact quantum evolution of the Husimi function (top) is compared to the classical Liouvillian dynamics (middle) and to the dynamics of a classical phase space ensemble (bottom).

#### IV. BREAKDOWN OF THE MEAN-FIELD APPROXIMATION

The phase-space description of the Bose-Hubbard model is especially suited to explore the correspondence of the quasi-classical mean-field approximation and the many-particle quantum dynamics. The established derivations of the Gross-Pitaevskii equation assumes a fully coherent quantum state, so that the mean-field approximation is restricted to this class of quantum states. In fact it has been shown that the approximation is no longer valid if the Gross-Pitaevskii dynamics becomes classically unstable [17, 18]. A particular illustrative example of this effect was introduced by Anglin and Vardi [11, 21], who demonstrated the breakdown of the mean-field approximation for a two-mode BEC around the hyperbolic fixed point shown in Fig. 1 on the right-hand side. The top row of Fig. 6 shows the resulting evolution of the quantum Husimi  $Q$ -function. Initially the system is in a fully condensed state, i.e. a  $SU(2)$  coherent state at  $p_0 = 0.9045$  and  $q_0 = 0$ , and thus the Husimi function is maximally localized. In the course of time the condensate approaches the hyperbolic fixed point, where the Husimi function rapidly diffuses along the unstable classical manifold. The coherence is lost and the Gross-Pitaevskii equation is no longer valid. This is further illustrated in Fig. 7, where the evolution of the quantum Bloch vector  $\langle \hat{\mathbf{J}} \rangle / N$  (solid blue line) is compared to its classical counterpart  $\mathbf{s}$  (solid red line). Both agree well in the beginning, when the system is fully condensed. However, the mean-field approximation breaks down as they approach the hyperbolic fixed point (marked by a cross

in the figure). The quantum Bloch vector penetrates into the Bloch sphere, while the classical vector  $\mathbf{s}$  is forced to remain on the surface.

However, this breakdown of the mean-field approximation is only due to the neglect of higher moments of the quantum state and not a consequence of a failure of the quasi-classical Gross-Pitaevskii dynamics. Thus it is easily resolved in quantum phase space. The middle row of Fig. 6 shows the evolution of a classical phase space distribution propagated by the Liouville equation (18) which coincides with the Husimi function at  $t = 0$ . With increasing particle number  $N$  the width of the initial distribution decreases such that one recovers a single phase space point in the macroscopic limit  $N \rightarrow \infty$ . One observes that the classical distribution captures the essential features of the quantum evolution – the spreading along the unstable manifold of the hyperbolic fixed point. Due to the neglect of the second order differential term in Eqn. (14) this spreading is a little overestimated while the quantum spreading in the orthogonal direction is absent. Thus, this can be construed as a disregard of quantum noise which guarantees the uncertainty relation. Furthermore we can interpret the Liouvillian flow in terms a classical phase space ensemble as shown in the bottom row of Fig. 6. At  $t = 0$  this ensemble is generated by 200 phase space points to mimic the quantum Husimi distribution. Afterwards all trajectories evolve according to the Gross-Pitaevskii equation (21) resp. (20). Fig. 7 shows the quasi-classical expectation value of the Bloch vector (dashed green line) calculated by the simple phase space average (16) in comparison to the quantum Bloch vector  $\langle \hat{\mathbf{J}} \rangle / N$ . One observes an ex-

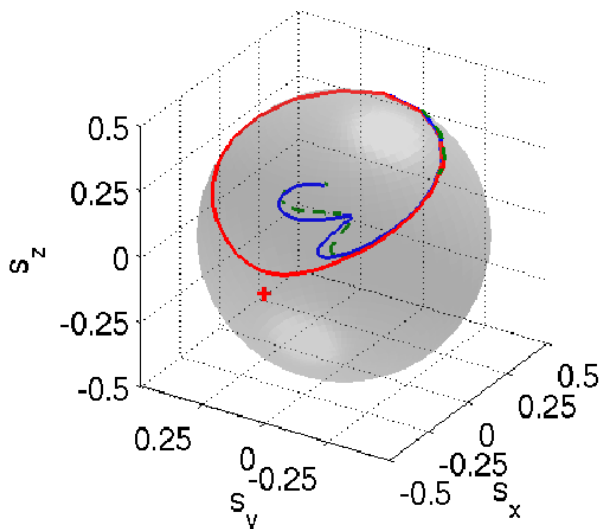


FIG. 7: (Color online) Time evolution of the Bloch vector  $\langle \hat{\mathbf{J}} \rangle / N$  approaching the hyperbolic fixed point (solid blue line) for the same parameters as in Fig. 6. The ensemble average over 500 trajectories (dashed green line) closely follows the quantum result, while a single trajectory (solid red line) breaks away in the vicinity of the hyperbolic fixed point (marked by a cross).

cellent agreement. Note that the expectation values calculated from the classical distribution function and the phase space ensemble are indistinguishable on this scale and thus only one curve is seen in the figure.

Finally we want to point out that the phase space picture also provides a quasi-classical description of genuine many-particle quantities. For instance we consider the condensate fraction of a many-particle quantum state, which can be defined as the leading eigenvalue of the reduced single-particle reduced density matrix (SPDM) [22]

$$\begin{aligned} \rho_{\text{red}} &= \frac{1}{N} \begin{pmatrix} \langle \hat{a}_1^\dagger \hat{a}_1 \rangle & \langle \hat{a}_1^\dagger \hat{a}_2 \rangle \\ \langle \hat{a}_2^\dagger \hat{a}_1 \rangle & \langle \hat{a}_2^\dagger \hat{a}_2 \rangle \end{pmatrix} \\ &= \frac{1}{N} \begin{pmatrix} N/2 - \langle \hat{J}_z \rangle & \langle \hat{J}_x \rangle - i \langle \hat{J}_y \rangle \\ \langle \hat{J}_x \rangle + i \langle \hat{J}_y \rangle & N/2 + \langle \hat{J}_z \rangle \end{pmatrix}. \end{aligned} \quad (23)$$

As discussed above, the expectation value of the angular momentum operators can be calculated from the quasi-classical phase space distribution function  $\rho(p, q)$  in a good approximation. From these it is also possible to reconstruct the SPDM and thus calculate the condensate fraction completely classically. Furthermore, it is important to note that these quantities are not accessible within a single trajectory mean-field approach. To illustrate this issue we compare the eigenvalues of the SPDM from the quasi-classical Liouville approximation with the exact quantum results in Fig. 8. Initially one eigenvalue is unity, indicating a pure BEC equivalent to a product state with every particle in the same mode. This eigenvalue decreases rapidly when the Husimi func-

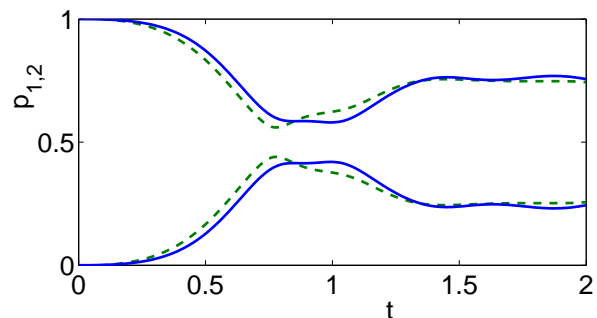


FIG. 8: (Color online) Eigenvalues of the reduced single-particle density matrix (23) calculated from the quantum (solid blue line) and the quasi-classical (dashed green line) Bloch vector depicted in Fig. 7.

tion approaches the hyperbolic fixed point (cf. Fig. 6), indicating a rapid depletion of the condensate mode. One observes that the classical calculation reproduces this depletion of the condensate mode very well.

## V. HEATING OF A TWO-MODE BEC

Recently, the long-time dynamics of a BEC interacting with the background gas has attracted a lot of interest [7, 23]. It was shown that collisions with the background gas lead to a decrease of the coherence of the two condensate modes, which can be used as a noise thermometer at extremely low temperatures. In this section we want to discuss the heating of a BEC within the quasi-classical phase space picture.

The main source of decoherence and heating is caused by collisions with the background gas atoms and can be described in leading order by the master equation [24, 25]

$$\begin{aligned} \dot{\hat{\rho}} &= -i[\hat{H}, \hat{\rho}] - \frac{\gamma_1}{2} \sum_{j=1,2} \hat{n}_j^2 \hat{\rho} + \hat{\rho} \hat{n}_j^2 - 2\hat{n}_j \hat{\rho} \hat{n}_j \\ &\quad - \frac{\gamma_2}{2} \sum_{j=1,2} \hat{a}_j \hat{a}_j^\dagger \hat{\rho} + \hat{\rho} \hat{a}_j \hat{a}_j^\dagger - 2\hat{a}_j^\dagger \hat{\rho} \hat{a}_j \\ &\quad - \frac{\gamma_2}{2} e^{\beta(\hbar\delta - \mu)/2} \sum_{j=1,2} \hat{a}_j^\dagger \hat{a}_j \hat{\rho} + \hat{\rho} \hat{a}_j^\dagger \hat{a}_j - 2\hat{a}_j \hat{\rho} \hat{a}_j^\dagger, \end{aligned} \quad (24)$$

where  $\mu$  is the chemical potential and  $\delta$  is the energy gap between the ground and the first excited mode of the trapping potential. The first terms describe elastic scattering events that conserve the number of particles in the condensate mode and only lead to phase decoherence (see, e.g., [26]). Thus they are readily described within the number conserving phase space approach discussed in the present paper, where the interpretation as phase noise becomes especially clear. The second contribution describes inelastic scattering of atoms in and out of the condensate. As argued in [25] this effect is smaller by orders of magnitude for certain trap geometries if the temperatures are low enough and only the



ground mode is occupied in every well. Thus we will neglect this amplitude decoherence effect, i.e. we set  $\gamma_2 = 0$  in the following.

The effects of the scattering events are conveniently understood and visualized in quantum phase space. The evolution equation for the Husimi function is obtained as in Sec. II by taking the expectation value in  $SU(2)$  coherent states:

$$\begin{aligned} \frac{\partial}{\partial t} Q(p, q) &= \langle p, q | \dot{\hat{\rho}} | p, q \rangle \\ &= i \operatorname{tr} \left( \hat{H} \hat{\rho} - \hat{\rho} \hat{H} | p, q \right) \langle p, q | \\ &\quad - \frac{\gamma_1}{2} \sum_{j=1,2} \operatorname{tr} \left( \hat{n}_j^2 \hat{\rho} + \hat{\rho} \hat{n}_j^2 - 2 \hat{n}_j \hat{\rho} n_j | p, q \right) \langle p, q | \end{aligned} \quad (25)$$

Using the  $\mathcal{D}$ -algebra representation of the operators introduced above, this equation can be cast into the form

$$\begin{aligned} \frac{\partial}{\partial t} Q(p, q) &= -2 \operatorname{Im}(\mathcal{D}^\ell(\hat{H})) Q(p, q) \\ &\quad - \frac{\gamma_1}{2} \sum_{j=1,2} (\mathcal{D}^\ell(\hat{n}_j) - \mathcal{D}^\ell(\hat{n}_j)^*)^2 Q(p, q) \\ &= -\{\mathcal{H}(p, q), Q(p, q)\} \\ &\quad - 2Up(1-p) \frac{\partial^2}{\partial p \partial q} Q(p, q) + \gamma_1 \frac{\partial^2}{\partial q^2} Q(p, q), \end{aligned} \quad (26)$$

with the classical Hamiltonian function (19). By an analogous calculation one finds the evolution equation for the Glauber-Sudarshan distribution:

$$\begin{aligned} \frac{\partial}{\partial t} P(p, q) &= -\{\mathcal{H}(p, q), P(p, q)\} \\ &\quad + 2Up(1-p) \frac{\partial^2}{\partial p \partial q} P(p, q) + \gamma_1 \frac{\partial^2}{\partial q^2} P(p, q), \end{aligned} \quad (27)$$

keeping in mind that the macroscopic interaction strength is now given by  $\tilde{g} = U(N+2)$  instead of  $g = UN$ . In these representations the effect of the decoherence term  $\sim \gamma_1$  becomes most obvious: It leads to a diffusion of the relative phase of the two condensates and thus to a blurring of the coherence of the two condensates modes. This effect has been directly measured in the experiments of the Oberthaler group [7, 23].

If we neglect the quantum noise term  $\sim g/N$ , the equations (27) and (28) reduce to Fokker-Planck equations. Thus the condensate dynamics can again be interpreted in terms of phase space ensembles, now subject to the stochastic evolution equations

$$\dot{p} = -\frac{\partial \mathcal{H}}{\partial q} \quad \text{and} \quad \dot{q} = +\frac{\partial \mathcal{H}}{\partial p} + \sqrt{2\gamma_1} \xi(t), \quad (28)$$

where  $\xi(t)$  describes uncorrelated white noise:

$$\langle \xi(t) \rangle = 0 \quad \text{and} \quad \langle \xi(t) \xi(t') \rangle = \delta(t - t'). \quad (29)$$

An example for this quasi-classical description of phase diffusion due to heating of the condensate is shown in

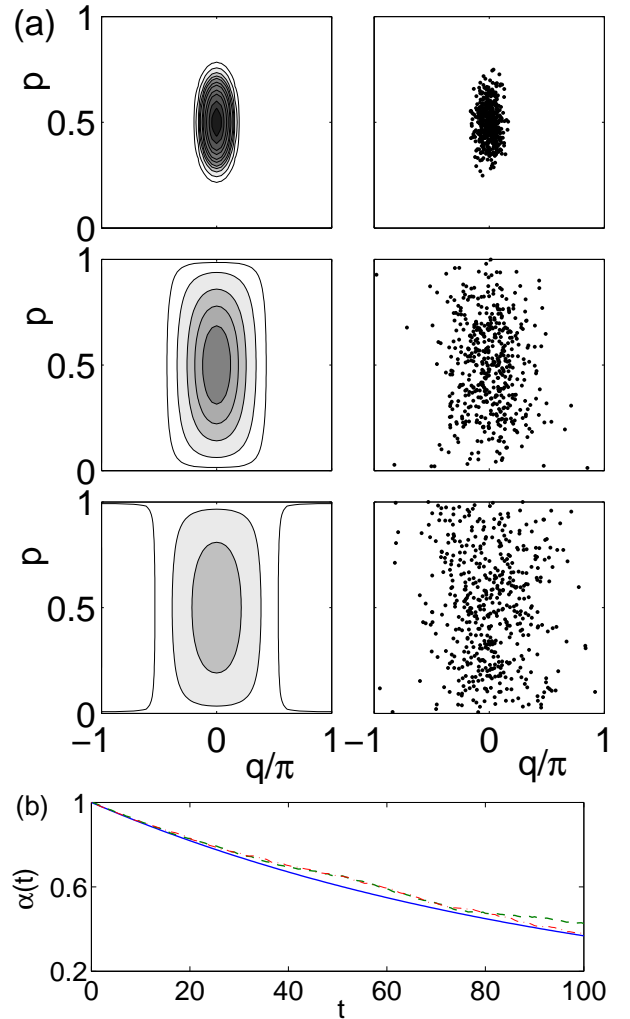


FIG. 9: Heating of a two-mode BEC in quantum phase space for  $UN = 0$ ,  $J = 1$ ,  $\epsilon = 0$  and  $\gamma_1 = 0.01$ . (a) Comparison of the exact quantum evolution of the Husimi function  $Q(p, q, t)$  (left-hand side) and the stochastic dynamics of a classical phase space ensemble (right-hand side) for  $t = 0, 30, 60$  (from bottom to top). Dark colors encode high values of the Husimi density. (b) Decay of the coherence factor  $\alpha(t)$ . The exact quantum result (solid blue line) is compared to ensemble simulations based on the  $Q$ -function (dashed green line) and the  $P$ -function (dash-dotted red line).

Fig. 9(a) for  $UN = 0$  and Fig. 10(a) for  $UN = 10$ , respectively. The left hand side shows the exact quantum evolution of the Husimi distribution  $Q(p, q, t)$  calculated from the evolution of the density matrix  $\hat{\rho}(t)$  according to the master equation (24). At  $t = 0$  the system is assumed to be in a coherent state  $|p = 1/2, q = 0\rangle$ , i.e., a pure condensate with equal population and zero phase difference between the two wells. In the course of time, the Husimi function spreads and thus the coherence factor  $\alpha(t) = \frac{2}{N} \langle \hat{J}_x \rangle_t$  decays as shown in part (b) of the figures. The right-hand sides of Fig. 9(a) and Fig. 10(a) show the evolution of a classical phase space ensemble initially distributed according to the Husimi function  $Q(p, q, 0)$ .



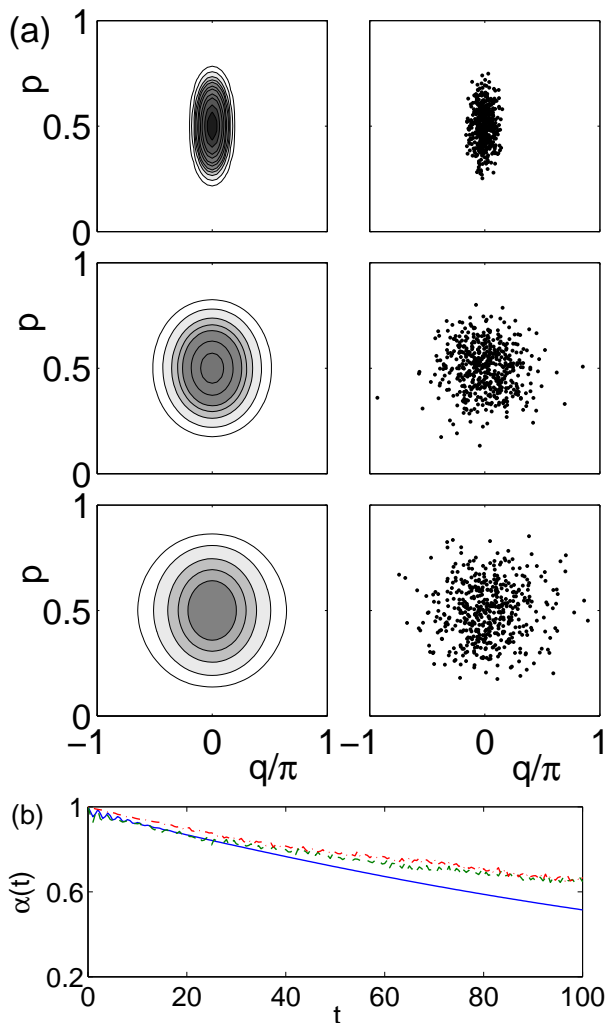


FIG. 10: As Fig. 9, however for  $UN = 10$ .

The single trajectories evolve according to the stochastic equations of motion (28) and thus diffuse over the classical phase space. One observes that the quantum dynamics is well reproduced by the classical approach, especially the different shape of the Husimi function for  $U = 0$  and  $U = 10$  after the diffusion process.

For a more quantitative analysis we have plotted the coherence factor  $\alpha(t)$  in Fig. 9(b) and Fig. 10(b). The quantum result  $\frac{2}{N} \langle \hat{J}_x \rangle_t$  is compared to the ensemble averages (16) over 500 classical trajectories for the  $Q$ -function and  $P$ -function, respectively. In the linear case  $UN = 0$  the mapping to stochastic evolution equations is exact and thus the deviations only result from the finite number of classical representations. For  $UN = 10$ , however, quantum noise is neglected leading to a systematic underestimation of loss of phase coherence.

Furthermore one observes that the coherence factor  $\alpha(t)$  decreases much slower for  $UN = 10$  compared to the non-interacting case  $UN = 0$  both in the exact and in the classical calculation. This difference is readily understood from the structure of the classical phase space

as shown in Fig. 1. One observes that the minimum of the classical Hamiltonian function  $\mathcal{H}(p, q)$  is much deeper for  $UN = 10$ , so that the classical trajectories are bound much stronger and phase diffusion is significantly reduced.

## VI. CONCLUSION AND OUTLOOK

In the present paper we have discussed the number-conserving phase space description of the Bose-Hubbard model for the simplest model system consisting of just two wells. Apart from its theoretic value as an highly illustrative model this system has attracted considerable experimental interest within the last years [5, 7].

We demonstrated the advantages of the Husimi phase space quasi-density for the analysis and discussion of quantum states. This representation allows a straightforward comparison of the many-body quantum system and its 'classical' counterpart given by the celebrated Gross-Pitaevskii equation. In fact the quantum eigenstates localize on the classical phase space trajectories.

The most important conclusion of the present paper is that two steps of approximation are necessary to derive the celebrated Gross-Pitaevskii equation for the dynamics of a Bose-Einstein condensate: Firstly the neglect of quantum fluctuations in the limit of many particles and secondly the assumption of a many-body quantum state strongly localized in phase space, i.e., a nearly pure BEC. For arbitrary quantum states one can still simulate the dynamics 'classically', however one now has to consider phase space densities propagating according to the classical Liouville equation or, equivalently, ensembles of phase space trajectories. We have demonstrated this issue for a BEC approaching a classically unstable fixed point. The condensate fraction rapidly decreases so that the dynamics cannot be described by a single GPE-trajectory any longer. This failure has been denoted as the breakdown of the mean-field approximation in the literature [11, 21]. We have shown that this is an artifact of the description by one point in quantum phase space. The breakdown can be cured by the introduction of classical phase space densities or ensembles.

Furthermore we have also discussed the heating of a BEC due to collisions with background gas atoms starting from a master equation description. It was shown that this effect can also be well understood in quantum phase space since the collisions lead to a diffusion of the relative phase of the two modes. Using this description it is easy to understand the dependence of the decoherence on the system parameters simply from the structure of the classical phase space.

Most of these facts are well established for a flat phase space in terms of Glauber coherent states but relatively unknown for systems with a constant of motion such as the particle number  $N$  in the present paper. The great advantage of this approach is that the particle number  $N$  appears as a parameter instead of an operator which

simplifies approximations and expansions in this quantity drastically. By a comparison with the well known evolution equations for phase space densities in single-particle quantum mechanics one can directly see the analogies between the classical limit and the macroscopic limit of many-body quantum mechanics. In this respect the inverse particle number  $1/N$  takes over the role of  $\hbar$  as a semiclassical parameter [27].

The introduction of coherent states and phase space distributions opens the door for the use of semiclassical methods for the Bose-Hubbard model. First of all we would like to stress that the method is not at all restricted to two modes. In the first part of the present work [4] we have introduced the phase space description and calculated the equations of motion for an arbitrary number of modes. The generalization of the ensemble method to this case is straightforward and allows the approximate calculation of many-particle quantities such as the condensate fraction or higher moments with small numerical efforts. Here we have restricted ourselves to the simplest

case just for didactic reasons. The 'classical' ensemble approach is of course not capable to describe generic quantum effect such as tunneling in quantum phase space and (self-)interference. These features can be reconstructed using semiclassical coherent state propagators, requiring however the generalization of techniques that have been established for flat phase space [28]. Further opportunities include the use of phase space entropies on spherical phase spaces (see, e.g., [20, 29]) to classify quantum states and entanglement.

### Acknowledgments

Support from the Studienstiftung des deutschen Volkes and the Deutsche Forschungsgemeinschaft via the Graduiertenkolleg "Nichtlineare Optik und Ultrakurzzeitphysik" is gratefully acknowledged.

- 
- [1] M. P. A. Fisher, P. B. Weichman, G. Grinstein, and D. S. Fisher, *Phys. Rev. B* **40**, 546 (1989).
  - [2] L. Pitaevskii and S. Stringari, *Bose-Einstein Condensation* (Oxford University Press, Oxford, 2003).
  - [3] C. Brif and A. Mann, *Phys. Rev. A* **59**, 971 (1999).
  - [4] F. Trimborn, D. Witthaut, and H. J. Korsch, arXiv:0802.1139.
  - [5] M. Albiez, R. Gati, J. Fölling, S. Hunsmann, M. Cristiani, and M. K. Oberthaler, *Phys. Rev. Lett.* **95**, 010402 (2005).
  - [6] T. Schumm, S. Hofferberth, L. M. Andersson, S. Wildermuth, S. Groth, I. Bar-Joseph, J. Schmiedmayer, and P. Krüger, *Nature Physics* **1**, 57 (2005).
  - [7] R. Gati, B. Hemmerling, J. Fölling, M. Albiez, and M. K. Oberthaler, *Phys. Rev. Lett.* **96**, 130404 (2006).
  - [8] C. Orzel, A. K. Tuchman, M. L. Fenselau, M. Yasuda, and M. A. Kasevich, *Science* **291**, 2386 (2001).
  - [9] G. J. Milburn, J. Corney, E. M. Wright, and D. F. Walls, *Phys. Rev. A* **55**, 4318 (1997).
  - [10] A. Smerzi, S. Fantoni, S. Giovanazzi, and S. R. Shenoy, *Phys. Rev. Lett.* **79**, 4950 (1997).
  - [11] A. Vardi and J. R. Anglin, *Phys. Rev. Lett.* **86**, 568 (2001).
  - [12] W.-M. Zhang, D. H. Feng, and R. Gilmore, *Rev. Mod. Phys.* **62**, 867 (1990).
  - [13] A. M. Perelomov, *Generalized Coherent States and Their Applications* (Springer, Berlin Heidelberg New York London Paris Tokyo, 1986).
  - [14] A. B. Klimov, *Journal of Mathematical Physics* **43**, 2202 (2002).
  - [15] D. Zueco and I. Calvo, *J. Phys. A* **40**, 4635 (2007).
  - [16] M. J. Steel, M. K. Olsen, L. I. Plimak, P. D. Drummond, S. M. Tan, M. J. Collett, D. F. Walls, and R. Graham, *Phys. Rev. A* **58**, 4824 (1998).
  - [17] Y. Castin and R. Dum, *Phys. Rev. Lett.* **79**, 3553 (1997).
  - [18] Y. Castin and R. Dum, *Phys. Rev. A* **57**, 3008 (1998).
  - [19] G.-B. Jo, Y. Shin, S. Will, T. A. Pasquini, M. Saba, W. Ketterle, D. E. Pritchard, M. Vengalattore, and M. Prentiss, *Phys. Rev. Lett.* **98**, 030407 (2007).
  - [20] S. Gnutzmann and K. Zyczkowski, *J. Phys. A* **34**, 10123 (2001).
  - [21] J. R. Anglin and A. Vardi, *Phys. Rev. A* **64**, 013605 (2001).
  - [22] A. J. Leggett, *Rev. Mod. Phys.* **73**, 307 (2001).
  - [23] R. Gati, J. Esteve, B. Hemmerling, T.B. Ottenstein, J. Appmeier, A. Weller, and M. K. Oberthaler, *New J. Phys.* **8**, 189 (2006).
  - [24] J. Anglin, *Phys. Rev. Lett.* **79**, 6 (1997).
  - [25] J. Ruostekoski and D. F. Walls, *Phys. Rev. A* **58**, R50 (1998).
  - [26] D. F. Walls and G. J. Milburn, *Phys. Rev. A* **31**, 2403 (1985).
  - [27] E. M. Graefe and H. J. Korsch, *Phys. Rev. A* **76**, 032116 (2007).
  - [28] M. Baranger, M. A. M. de Aguiar, F. Keck, H. J. Korsch, and B. Schellhaaß, *J. Phys. A* **34**, 7227 (2001).
  - [29] F. Mintert and K. Zyczkowski, *Phys. Rev. A* **69**, 022317 (2004).